



# Synthesis of Novel Oxazolo[4,5-b]pyridine-2-one based 1,2,3-triazoles as Glycogen Synthase Kinase-3 $\beta$ Inhibitors with Anti-inflammatory Potential

Mushtaq A. Tantray<sup>1</sup>, Imran Khan<sup>1</sup>,  
Hinna Hamid<sup>1,\*</sup>, Mohammad Sarwar Alam<sup>1</sup>,  
Sadiq Umar<sup>2</sup>, Yakub Ali<sup>1</sup>, Kalicharan Sharma<sup>3</sup>  
and Firasat Hussain<sup>4</sup>

<sup>1</sup>Department of Chemistry, Faculty of Science, Hamdard University (Jamia Hamdard), New Delhi 110 062, India

<sup>2</sup>Department of Pharmaceutical Sciences, College of Pharmacy, Washington State University, Spokane, WA 99202, USA

<sup>3</sup>Drug Design and Medicinal Chemistry Lab, Department of Pharmaceutical Chemistry, Hamdard University (Jamia Hamdard), New Delhi 110 062, India

<sup>4</sup>Department of Chemistry, University of Delhi, New Delhi 110 007, India

\*Corresponding author: Hinna Hamid,  
hhamid@jamiahamdard.ac.in

A novel series of oxazolo[4,5-b]pyridine-2-one based 1,2,3-triazoles has been synthesized by click chemistry approach and evaluated for *in vitro* GSK-3 $\beta$  inhibitory activity. Compound 4g showed maximum inhibition with IC<sub>50</sub> value of 0.19  $\mu$ M. Keeping in view the effect of GSK-3 $\beta$  inhibition on inflammation, compounds 4g, 4d, 4f, 4i, 4n and 4q exhibiting significant GSK-3 $\beta$  inhibition were examined for *in vivo* anti-inflammatory activity in rat paw edema model. The compounds 4g, 4d, 4f and 4i showed pronounced *in vivo* anti-inflammatory activity (76.36, 74.54, 72.72 and 70.90%, respectively, after 5h post-carrageenan administration) and were further found to inhibit the pro-inflammatory mediators, viz. NO, TNF- $\alpha$ , IL-1 $\beta$ , and IL-6 substantially in comparison with indomethacin, an anti-inflammatory drug as well as SB216763, a GSK-3 $\beta$  inhibitor, reported to exert a similar effect. Histopathology studies confirmed the tolerance of gastric mucosa to these compounds.

**Key words:** click chemistry, glycogen synthase kinase-3, inflammation, oxazolo[4,5-b]pyridine-2-one, pro-inflammatory mediators

Received 23 October 2015, revised 6 January 2016 and accepted for publication 16 January 2016

Glycogen synthase kinase-3 (GSK-3) is a ubiquitous multifunctional serine/threonine kinase, originally identified by

virtue of regulating glycogen metabolism. GSK-3 exists as two major isoforms in mammals, GSK-3 $\alpha$  and GSK-3 $\beta$ . Both are ubiquitously expressed in all tissues and share an overall homology of 85%, with 98% homology within their kinase domains (1). GSK-3 $\beta$  is the more conserved isoform in evolution with wide expression throughout the animal kingdom, while GSK-3 $\alpha$  is only found in vertebrates (2). GSK-3 has been recognized to modulate a diverse array of key regulatory intra-cellular proteins such as metabolic proteins (e.g. cyclin D1, APP, and presenilin), structural proteins (e.g. tau and other microtubule associated proteins) and transcription factors (e.g. NF- $\kappa$ B, p53 and Notch) (3,4). The plethora of substrates enable GSK-3 to determine the output of various signaling pathways initiated by diverse stimuli (5). Deregulation of GSK-3 activity and its associated signaling pathways results in the development of several human diseases as type II diabetes, bipolar disorder, cancer, chronic inflammatory diseases, and Alzheimer's disease (AD) (6–9). Given its unique position, GSK-3 has gained a spotlight status as an interesting therapeutic target and a means to unravel the molecular basis of its associated disorders (10). Inhibition of GSK-3, thus, represents a plausible strategy to develop novel drug therapy for the treatment of such pathologies.

GSK-3 $\beta$  is also a crucial mediator of inflammation. The paramount importance of GSK-3 $\beta$  in controlling inflammation is evident by its capacity to modulate the inflammatory response in both innate and adaptive immune cells (1). Numerous transcription factors such as NF- $\kappa$ B necessary for controlling acute inflammation act as substrates of GSK-3 $\beta$  and are responsible for production of various pro-inflammatory mediators such as TNF- $\alpha$ , IL-1 $\beta$ , iNOS, and IL-6 (11,12). Inhibition of GSK-3 $\beta$  controls inflammation and protects the host against inflammatory-mediated pathology and death in animal models. GSK-3 $\beta$  inhibitors have been reported to suppress inflammation in various animal models against TNF- $\alpha$  administration, endotoxemia, experimental colitis, type II collagen-induced arthritis, ovalbumin-induced asthma, carrageenan induced lung injury, and experimental autoimmune encephalomyelitis (11,13–22). The development of GSK-3 $\beta$  inhibitors may thus provide an important therapeutic approach for the treatment of inflammatory diseases. Also, as various other pathologies such as diabetes, cancer, and AD linked to abnormal functioning of GSK-3 are associated with



inflammation, the inhibitors of GSK-3 $\beta$  may provide therapeutic anti-inflammatory effects in a broad range of conditions (23).

In continuation to the work performed by our group on benzoxazolinone and 2-mercaptobenzoxazole-based 1,2,3-triazole conjugates as anti-inflammatory compounds (24–26), we extended our studies to oxazolo[4,5-b]pyridine-2-one moiety, the bio-isostere of benzoxazolinone and 2-mercaptobenzoxazole. Oxazolopyridinones have been reported to be pharmaceutically important as anti-nociceptive, anti-inflammatory, anti-malarial, and Met kinase inhibitors (27–33). Recently, oxazolo-pyridines have also been reported as potent GSK-3 $\beta$  inhibitors (34). So far not much work has been performed on this scaffold and there is ample scope for the development of more potent inhibitors from this ligand. Similarly 1,2,3-triazoles and their derivatives have received considerable attention due to their role in diverse biological activities such as antimicrobial, anti-inflammatory, local anesthetic, anticonvulsant, anti-neoplastic, antimalarial, and antiviral activities (35,36). 1,2,3-triazole moiety has also been reported as a novel class of selective GSK-3 $\beta$  inhibitors (37). We therefore focused our attention on the development of novel oxazolo[4,5-b]pyridine-2-one based GSK-3 inhibitors by conjugating them to 1,2,3-triazoles through a click chemistry approach. The aim of the work was to develop molecules having GSK-3 $\beta$  inhibitory activity with anti-inflammatory properties. A library of 21 compounds has been synthesized and evaluated for *in vitro* GSK-3 $\beta$  inhibition and *in vivo* anti-inflammatory activity. The compounds exhibiting significant GSK-3 $\beta$  inhibition and anti-inflammatory profile have been further evaluated for their effect on pro-inflammatory mediators such as NO, TNF- $\alpha$ , IL-1 $\beta$ , and IL-6, using *ex vivo* assays. *In silico* molecular docking studies of the active compounds were also carried out against GSK-3 $\beta$  to get an insight into the molecular interactions of these compounds with its active site. Furthermore, as the anti-inflammatory compounds are known to cause gastric ulceration as side effect, the active compounds have been assessed for their gastric ulceration risk.

## Experimental

### Chemistry

The synthetic procedure and the characterization data of target compounds (**4a–4u**) has been provided in the Appendix S1.

### Pharmacology

#### Chemicals

Human recombinant glycogen synthase kinase-3 $\beta$  and pre-phosphorylated polypeptide substrate glycogen synthase-2 (GS-2) were purchased from Merck-Millipore

## Oxazolopyridinone-triazoles as GSK-3 $\beta$ Inhibitors

Corporation (New Delhi, India). Kinase-Glo Luminescent Kinase Assay (catalog no. V6713) was obtained from Promega Corporation (Madison, WI, USA). Indomethacin, Carrageenan, Carboxymethylcellulose, Lipopolysaccharide (LPS), Lithium chloride, and Staurosporine were purchased from Sigma-Aldrich Chemicals Pvt. Limited, Bangalore, India.

### GSK-3 $\beta$ inhibitory activity

The synthesized compounds were screened for their GSK-3 $\beta$  inhibition as per the Kinase-Glo assay method of Baki *et al.* (38). The sensitivity of the assay is comparable to the radioactive method. This assay determines the kinase activity by quantifying the amount of ATP remaining in solution following a kinase reaction. In a typical assay, 10  $\mu$ L of test compound of different concentrations (dissolved in dimethyl sulfoxide [DMSO] and diluted with assay buffer) and 10  $\mu$ L (20 ng) of enzyme were added to each well followed by 20  $\mu$ L of assay buffer containing substrate and ATP to get a concentration of 25  $\mu$ M substrate and 1  $\mu$ M ATP per well. The final DMSO concentration in the reaction mixture was <1%. After incubation at 30 °C for 30 min, the enzymatic reaction was quenched with 40  $\mu$ L of Kinase-Glo reagent. Luminescence was recorded after 10 min using Infinite F200<sup>®</sup> PRO multimode reader (Tecan Group Ltd., Männedorf, Switzerland). The activity is proportional to the difference of the total and consumed ATP. Maximum activity was found in the absence of inhibitor and was used to calculate the inhibitory activities of test compounds. Staurosporine was used as a standard GSK-3 $\beta$  inhibitor.

### Animals

Wistar rats of either sex (150–200 g) were obtained from Central Animal House, Hamdard University, New Delhi. They were kept in the Central Animal House of Hamdard University in colony cages at an ambient temperature of 25  $\pm$  2 °C and relative humidity 45–55% with 12 h light/dark cycles after initial acclimatization for about 1 week. They had free access to standard rodent pellet diet and water *ad libitum*. Fourteen hours prior to the start of the experiment, the animals were sent to laboratory and fed only with water *ad libitum*. The experimental study was conducted in accordance with the Institutional Animal Ethics Committee of the University, Jamia Hamdard, New Delhi, India.

### Anti-inflammatory activity

The synthesized compounds were evaluated for their *in vivo* anti-inflammatory activity using carrageenan-induced hind paw edema method. The rat paw edema was induced by injection of 0.1 mL of 1% freshly prepared saline solution (39) of carrageenan subcutaneously into the sub-plantar region of the right hind paw of rats. The standard anti-inflammatory drug, indomethacin (20 mg/kg

BW), was given orally as a positive control. GSK-3 $\beta$  inhibitor, SB216763 (20 mg/kg BW), was also administered to one group orally. The control group was only administered with 0.1 mL of 0.9% saline solution orally. The test groups were given the synthesized compounds orally at a dosage of 20 mg/kg BW, 1 h preceding the carrageenan administration. The paw volumes were measured at an interval of 3 and 5 h using plethysmometer (40).

#### Lipopolysaccharide (LPS)-induction into rat paw

Wistar albino rats weighing 150–200 g were used. Rats were fasted for 18 h before i.p. dosing with the test compound. The standard drug indomethacin (10  $\mu$ M) and GSK-3 $\beta$  inhibitor SB216763 (10  $\mu$ M) were given orally as a positive control. The control group was administered orally with 0.9% of 0.1 mL of saline solution only. The test groups were administered orally with the synthesized compounds at 20  $\mu$ M, 2 h before an intra-planter injection of LPS into rat paw. Following dosing of drugs, rats were injected with 50  $\mu$ L of saline containing 10  $\mu$ g/paw LPS. Two hours later, inflamed rat paw were collected from the inflamed animals (41,42).

#### Measurement of Nitric oxide (NO) level

After the experiment, animals were sacrificed and the hind paw tissues were washed with PBS (pH 7.4) and placed on ice by the method described earlier (43). Briefly a 50  $\mu$ L sample was added to 100  $\mu$ L of Griess reagent, and the reaction mixture was incubated for about 5–10 min at room temperature and protected from light. The optical density was measured at 540 nm in microplate reader as per the reagent manufacturer's protocol. Calculations were performed after generating a standard curve from sodium nitrite in the same buffer as used for preparation of homogenate.

#### Measurement of TNF- $\alpha$ IL-1 $\beta$ , and IL-6

Levels of inflammatory cytokines TNF- $\alpha$  IL-1 $\beta$ , and IL-6 in the serum were determined using commercially available cytokine ELISA kits (R&D and Cayman, Ann Arbor, MI, USA). Supernatants were removed and assayed in duplicate according to the manufacturer's guidelines. Cytokine concentrations were expressed as picograms of antigen per milliliter.

#### Docking studies

For better understanding of binding mode of substituted oxazolo pyridine-2-one derivatives at the molecular level, we carried out molecular docking simulations of synthesized molecules (**4d**, **4f**, **4g**, **4i**) at the GSK-3 $\beta$  catalytic ligand binding site. The docking simulations of synthesized compounds were performed using MAESTRO, version 9.4 implemented from SCHRODINGER software suite. The ligands were sketched in 3D format using build panel and were

prepared for docking using ligprep application. The protein for docking study was taken from Protein Data Bank (PDB ID: 4IQ6) and prepared by removing solvent, adding hydrogen, and further minimization in the presence of bound ligand (IQ6) using protein preparation wizard. Grids for molecular docking were generated with bound co-crystallized ligand. For the validation of docking parameters, the co-crystal ligand (IQ6) was re-docked at the catalytic site of protein and the RMSD between co-crystal and re-docked pose was found to be 0.255 Å. All compounds were docked using Glide extra-precision (XP) mode, with up to three poses saved per molecule.

#### Ulcerogenic activity

The compounds exhibiting significant anti-inflammatory activity were assessed further for their ulcerogenic risk evaluation (44). This was performed at 3-fold higher dose as compared to that used for anti-inflammatory activity. Each group constituted of three animals and were later sacrificed 5 h after oral drug administration. In comparison with indomethacin, the tested compounds were not found to cause any gastric ulceration and disruption of gastric epithelial cells at the given dose. SB216763 was also not found to cause any gastric ulceration. The gastric tolerance of these compounds toward the gastric mucosa was thus better than that of standard drug indomethacin.

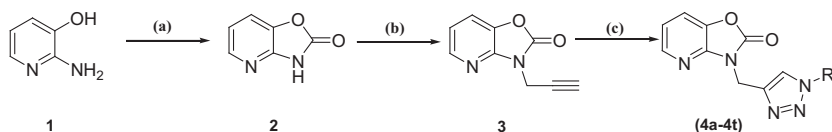
#### Statistical analysis

Results are expressed as the mean  $\pm$  SEM, and different groups were compared using one-way analysis of variance (ANOVA) followed by Tukey Kramer test for multiple comparisons.

## Results and Discussion

#### Chemistry

2-Amino-3-hydroxypyridine **1** was refluxed with 1,1-carbonyldiimidazole in dry THF for 5–6 h under nitrogen atmosphere to yield oxazolo[4,5-b]pyridin-2(3H)-one **2** as depicted in Scheme 1. It was then refluxed with propargyl bromide in presence of potassium carbonate in dry acetone for 4–5 h to obtain 3-ethynylloxazolo[4,5-b]pyridin-2(3H)-one **3**. The propargylated oxazolopyridinone **3** was subsequently treated with various aromatic azides under click chemistry conditions to afford the target compounds, oxazolo[4,5-b]pyridin-2(3H)-one based 1,2,3-triazoles (**4a–4u**) in quantitative yields (Table S1). The formation of propargylated intermediate **3** was validated by the appearance of singlets at  $\delta$  4.65 and  $\delta$  2.27 in the  $^1$ H-NMR spectrum, corresponding to methylene protons and terminal alkyne proton, respectively. Presence of a signal in the region of  $\delta$  8.58–9.10 due to H-C(5) of triazole ring confirmed the synthesis of triazoles. The  $^{13}$ C NMR spectra further confirmed the structural assignments, showing the C-atom signals corresponding to triazole derivatives. The final structure veri-



**Scheme 1:** Synthetic approach for novel oxazolo[4,5-b]pyridin-2(3H)-one based 1,2,3-triazoles. (a) 1,1'-Carbonyldiimidazole, THF, Reflux; (b) Propargyl bromide, K<sub>2</sub>CO<sub>3</sub>, Acetone, Reflux; (c) Azides (R-N<sub>3</sub>), CuSO<sub>4</sub>·5H<sub>2</sub>O, Sodium ascorbate, tBuOH: H<sub>2</sub>O (1:1), r.t.

fication was performed by ESI-MS analysis which showed the presence of [M]<sup>+</sup> or [M + 1]<sup>+</sup> or [M + 2]<sup>+</sup> ion peaks.

### In vitro GSK-3 $\beta$ inhibitory activity

All the synthesized oxazolopyridinone triazoles were evaluated for inhibition of GSK-3 $\beta$  by Kinase-Glo™ luminescent technique (38,45). The results as illustrated in Table S1 shows that the compounds inhibited GSK-3 $\beta$  in the submicromolar to micromolar range. Among these, compounds **4g**, **4d**, **4f**, and **4i** were found to be the most active with IC<sub>50</sub> values of 0.19, 0.23, 0.31 and 0.37  $\mu$ M, respectively. Compounds **4n**, **4q**, **4l**, and **4b** displayed moderate inhibition in single-digit micromolar range while as the rest of the compounds exhibited relatively weak inhibition.

### In vivo anti-inflammatory activity

In view of the nexus between GSK-3 $\beta$  inhibition and alleviation of inflammatory disorders, the reported anti-inflammatory potential of oxazolopyridinones and 1,2,3-triazoles, the synthesized compounds exhibiting significant GSK-3 $\beta$  inhibitory activity were also examined for their *in vivo* anti-inflammatory activity by carrageenan-induced hind paw edema model. Indomethacin, an anti-inflammatory drug was taken as standard. SB216763, a well-known GSK-3 $\beta$  inhibitor, reported to exert anti-inflammatory effect in various *in vitro* and *in vivo* models, was also used as the reference. As illustrated in Table S2 indicated that all the tested compounds showed a time-dependent increase in the inhibition of inflammation after 3 h and 5 h post-carrageenan administration. The compounds **4g** and **4d** exhibited significant anti-inflammatory potential (73.58 and 71.69% inhibition at 3 h and 76.36 and 74.54% inhibition, respectively, at 5 h post-carrageenan administration) comparable to that of indomethacin (79.24% at 3 h and 83.63% at 5 h after carrageenan administration). Compounds **4f** and **4i** also showed a fairly good profile, reducing the paw volume by 69.81% and 67.92% after 3 h interval and 72.72% and 70.90%, respectively, after 5 h interval, in comparison with indomethacin. However, compounds **4n** and **4q** displayed moderate activity. SB216763 was found to exhibit 75.47% inhibition at 3 h and 78.18% inhibition at 5 h post-carrageenan treatment in comparison with indomethacin.

To get a better picture, these results were compared with GSK-3 $\beta$  inhibitory data of these compounds. Compounds **4g**, **4d**, **4f**, and **4i** were found to possess significant activ-

ity against both GSK-3 $\beta$  as well as *in vivo* induced inflammation. Moreover, the anti-inflammatory activity of the tested compounds was observed to be in conformity with their GSK-3 $\beta$  inhibition profile. The compounds, therefore, displayed good coordination between GSK-3 $\beta$  inhibition and anti-inflammatory property, that is, compounds inhibiting GSK-3 $\beta$  also reduced inflammation, indicating the role GSK-3 $\beta$  inhibitors can play against inflammation and inflammatory associated conditions.

### Effect of compounds **4g**, **4d**, **4f**, and **4i** on pro-inflammatory mediator levels

Pro-inflammatory cytokines such as TNF- $\alpha$ , IL-1 $\beta$  as well as IL-6 have a central role in the perpetuation of chronic inflammation and tissue damage during progression of inflammatory disorders. Blockade of these molecules result in a reduction of disease severity (46). As GSK-3 $\beta$  inhibitors such as lithium chloride, SB216763, TDZD8, and CHIR99021 have been reported to suppress inflammation by inhibiting the production of pro-inflammatory cytokines and increasing anti-inflammatory cytokine production, compounds **4g**, **4d**, **4f**, and **4i** exhibiting significant *in vivo* anti-inflammatory potential were, therefore, examined for their effect on concentration of various pro-inflammatory mediators.

### Nitric oxide

Nitric oxide (NO) is an important signaling molecule, produced as part of the inflammatory response from activated cells and macrophages (47,48). Huang *et al.* (19) have demonstrated that GSK-3 inhibition can block NO and iNOS production in response to LPS in primary microglia. In this study, increased NO levels have been detected in the LPS group similar with those previously reported in the literature (49). Analysis of nitrite estimation is summarized in Figure S1. A significant increase in nitrite was observed in LPS-induced inflammation group as compared to control. The treatment with synthesized compounds **4g**, **4d**, **4f**, and **4i** led to a decline in the nitrite level as compared to the inflammation group.

### Effect on IL-1 $\beta$ , TNF- $\alpha$ , and IL-6

During inflammatory processes, large amounts of the pro-inflammatory mediators are generated, which affect the immune system by suppressing the proliferation of T and B cells, as well as cytokine synthesis (50). IL-1 $\beta$  and TNF-

$\alpha$  stimulation upregulates the expression of pro-inflammatory genes, such as cyclooxygenase 2 (COX-2) and nitric oxide synthase (NOS). Takada *et al.* (21), showed LPS induced the production of these cytokines through glyco-gen synthase kinase-3 $\beta$ . Our results as depicted in Figure S2 showed that there is a significant increase in the level of TNF- $\alpha$ , IL-1 $\beta$ , and IL-6 in LPS-induced inflammation in experimental rats in comparison with control. Administration of selected compounds **4g**, **4i**, **4d**, and **4f** suppressed the increase in the level of TNF- $\alpha$ , IL-1 $\beta$ , and IL-6 significantly when compared to the LPS group.

### Molecular docking studies

To analyze the binding pattern of the active compounds (**4g**, **4d**, **4f**, and **4i**), molecular docking studies were performed against GSK-3 $\beta$ . The docking scores are shown in Table S3. Compound **4g** exhibited a docking score of -6.34 in comparison with that of the reference ligand IQ6 (6-chloro-N-cyclohexyl-4-(1H-pyrrolo[2,3-b]pyridin-3-yl)pyridin-2-amine), which showed a docking score of -9.86. The binding pose of compound **4g** and its comparison with the standard co-crystal ligand (IQ6) bonded to GSK-3 $\beta$  protein (PDBID: 4IQ6) is shown in Figure S3A–D. The oxazolopyridine-2-one moiety plays an important role in the binding, as the carbonyl oxygen atom is involved in hydrogen bonding interaction with backbone atom of the amino acid residue Val-135 in hinge region. The Val-135 residue has been known to contribute to equivalent hydrogen bonds in most of the GSK-3 $\beta$  inhibitor classes known including paullones, indirubin-3'-oxime, staurosporine, ARA-014418, maleimides, benzimidazoles, oxadiazoles, and pyrazolopyridine (51–53). Interaction with hinge region residues such as Val-135, Asp-133, and/or Tyr-134 is thus important for exhibiting potent GSK-3 $\beta$  inhibition (54). In addition, the phenyl ring of the triazole moiety exhibits  $\pi$ - $\pi$  stacking interaction with the phenyl ring (backbone) of the amino acid residue Phe-67 in the DFG motif region and hydrophobic interactions with GSK-3 $\beta$  protein Leu-188, Ileu-62, Val-70, and Ala-83 amino acid residues, interactions which are reported to determine selectivity as well potency for GSK-3 $\beta$  inhibition (54). These interactions probably explain the *in vitro* GSK-3 $\beta$  inhibitory activity exhibited by oxazolopyridine-2-one based 1,2,3-triazoles. We also compared the binding interactions of the most active compound **4g** with the co-crystallized ligand (IQ6) against the target site as shown in Figure S3E. Standard ligand IQ6 exhibits high docking score as it shows binding interaction with both Val 135 and Asp 133 in hinge region. This standard ligand also shows the binding interaction with Asp 200 in the DFG motif region. Some part of the ligand **4g** is partially superimposed with standard IQ6 in hinge region and shows the common interaction with Val 135. The difference in the GSK-3 $\beta$  inhibitory activity of the docked synthesized compounds (**4g**, **4d**, **4f**, and **4i**), may be mainly due to the lack of interaction with Asp-133 in the hinge region when compared to the standard.

### Ulcerogenic risk evaluation

The compounds showing potential anti-inflammatory activity were tested for their gastric ulcerogenic effect. As compared to indomethacin, SB216763 and the active compounds **4g**, **4d**, **4f**, and **4i** did not show any gastric ulceration and disruption of gastric epithelial cells at even three times higher dose than used for anti-inflammatory activity (Figure S4).

### Structure activity relationship

Based on the results, a preliminary structure–activity relationship was determined to correlate the effect of different structural features of synthesized compounds on the efficacy of their GSK-3 $\beta$  inhibition and anti-inflammatory properties.

- Compounds with substitution at ortho-position on the phenyl ring were found to be more active against both GSK-3 $\beta$  as well as induced inflammation in comparison with their corresponding para-substituted derivatives. Halo-substituted ortho derivatives were found to exhibit better activity in comparison with compounds having either alkyl or alkoxy substituents at ortho-position.
- Among the halo-substituted derivatives, chloro-substitution resulted in maximum activity followed by bromo- and fluoro-substitution at ortho-position. However, the order of activity at para-position was Br>Cl>F.
- Compounds possessing chloro group at either ortho- or para-position in the phenyl ring showed better activity than corresponding meta-substituted and di-substituted compounds.
- Substitution of alkyl groups on aromatic ring led to increase in activity than the substitution of corresponding alkoxy groups.
- Substitution of ethoxy group at para-position of aromatic ring reduced GSK-3 $\beta$  as well as *in vivo* inflammatory activity in comparison with substitution of methoxy group at the same position.
- Presence of bulky ter-butyl group at para-position of aromatic ring decreased the activity as compared to ethyl group at the corresponding position.
- Mono-alkyl substituted phenyl derivatives resulted in higher activity than dialkyl-substituted derivative.

### Crystallographic study

Intensity data were collected at 293(2) K an Oxford Xcalibur Sapphire 3 diffractometer (a single wavelength Enhance X-ray source with MoK $\alpha$  radiation,  $\lambda$  = 0.71073 Å) (57). The selected suitable single crystals



were mounted using paratone oil on the top of a glass fiber fixed on a goniometer head and immediately transferred to the diffractometer. Pre-experiment, data collection, data reduction, and analytical absorption corrections (58) were performed with the Oxford program suite *CrysAlisPro* (59). The crystal structures were solved with OLEX2.Solve (60) using direct methods. The structure refinements were performed by full-matrix least-squares on  $F^2$  with SHELXL-97 (61,62).

The chemical formula and ring labeling system are shown in Figure S5. Crystal data for compound **4q**:  $C_{16}H_{13}N_5O_3$ , Mr, 323.31; system, monoclinic; space group,  $P 2_1/n$ ; unit cell dimensions,  $a = 11.555(8) \text{ \AA}$ ;  $b = 9.048(4) \text{ \AA}$ ;  $c = 14.588(9) \text{ \AA}$ ;  $\beta = 97.89(6)^\circ$ ;  $V = 1510.7(16) \text{ \AA}^3$ ;  $Z = 4$ ;  $T = 293 \text{ K}$ ;  $R_{int}$ , 0.0375;  $R(\text{all})$ , 0.0943;  $Gof = 1.065$ ;  $\Delta\rho_{max} = 0.153 \text{ e \AA}^{-3}$ ;  $\Delta\rho_{min} = -0.114 \text{ e \AA}^{-3}$ .

Some of the hydrogen atoms were calculated after each cycle of refinement using a riding model, with C-H =  $0.93 \text{ \AA} + U_{iso}(H) = 1.2U_{eq}(C)$  for aromatic H atoms, with C-H =  $0.97 \text{ \AA} + U_{iso}(H) = 1.2U_{eq}(C)$  for methylene H atoms, C-H =  $0.97 \text{ \AA} + U_{iso}(H) = 1.5U_{eq}(C)$  for methyl H atoms.

Crystallographic data for the structure **4q** have been deposited with the Cambridge Crystallographic Data Center (CCDC) under the number CCDC-1431888. Copies of the data can be obtained, free of charge, on application to CCDC 12 Union Road, Cambridge CB2 1EZ, UK [Fax: +44-1223-336033; e-mail: deposit@ccdc.cam.ac.uk or at www.ccdc.cam.ac.uk].

## Conclusion

A focused library of novel compounds encompassing oxazo[4,5-b]pyridine-2-one scaffold conjugated through methylene linkage to 1,2,3-triazole fragment has been synthesized. The crystallographic study of the compound **4q** confirmed the formation of final molecule and supported the spectroscopic data. Given the association between GSK-3 $\beta$  inhibition and inflammation, compounds **4d**, **4f**, **4g**, **4i**, **4n**, and **4q** exhibiting significant GSK-3 $\beta$  inhibition were evaluated for *in vivo* anti-inflammatory activity in rat paw edema model. The compounds **4g**, **4d**, **4f**, and **4i** showing pronounced *in vivo* anti-inflammatory activities were further screened for the effect on pro-inflammatory mediators, NO, TNF- $\alpha$ , IL-1 $\beta$ , and IL-6. The compounds tested suppressed the production of these mediators significantly comparable to both indomethacin and SB216763, with **4g** showing maximum inhibition. Furthermore, the ulcerogenic risk evaluation of the active compounds showed their effective tolerance by gastric mucosa. These molecules may thus be considered as potent compounds possessing both GSK-3 $\beta$  inhibitory as well as anti-inflammatory property. Further exploration of the pathological implications of GSK-3 $\beta$  inhibition including inflammatory disorders by active compounds **4g**, **4d**, **4f**, and **4i** is being considered.

## Acknowledgments

The authors wish to express their thanks to Dr. G. N. Qazi, Vice-Chancellor, Jamia Hamdard for providing necessary facilities to carry out this work. The authors thank DST-SERB, Govt. of India, for awarding research project to HH and fellowship to IK. The author MAT is thankful to HNF for providing research assistance.

## Conflict of Interest

The authors report no conflict of interests.

## References

1. Wang H., Brown J., Martin M. (2011) Glycogen synthase kinase 3: a point of convergence for the host inflammatory response. *Cytokine*;53:130–140.
2. Alon L.T., Pietrokovski S., Barkan S., Avrahami L., Kaidanovich-Beilin O., Woodgett J.R., Barnea A., Eldar-Finkelman H. (2011) Selective loss of glycogen synthase kinase-3 $\alpha$  in birds reveals distinct roles for GSK-3 isozymes in tau phosphorylation. *FEBS Lett*;585:1158–1162.
3. Silva T., Reis J., Teixeira J., Borges F. (2014) Alzheimer's disease, enzyme targets and drug discovery struggles: from natural products to drug prototypes. *Ageing Res Rev*;15:116–145.
4. Del'Guidice T., Latapy C., Rampino A., Khlgatyan J., Lemasson M., Gelao B., Quarto T., Rizzo G., Barbeau A., Lamarre C., Bertolino A., Blasi G., Beaulieu J.-M. (2015) FXR1P is a GSK3 $\beta$  substrate regulating mood and emotion processing. *Proc Natl Acad Sci USA*;112: E4610–E4619.
5. Song W.J., Song E.A., Jung M.S., Choi S.H., Baik H.H., Jin B.K., Kim J.H., Chung S.H. (2015) Phosphorylation and inactivation of glycogen synthase kinase 3-beta (GSK3beta) by dual-specificity tyrosine phosphorylation-regulated kinase 1A (Dyrk1A). *J Biol Chem*;290:2321–2333.
6. Martinez A., Castro A., Dorronsoro I., Alonso M. (2002) Glycogen synthase kinase 3 (GSK-3) inhibitors as new promising drugs for diabetes, neurodegeneration, cancer, and inflammation. *Med Res Rev*;22:373–384.
7. Li B., Thrasher J.B., Terranova P. (2015) Glycogen synthase kinase-3: A potential preventive target for prostate cancer management. *Urol Oncol*;33:456–463.
8. Golpich M., Amini E., Hemmati F., Ibrahim N.M., Rahmani B., Mohamed Z., Raymond A.A., Dargahi L., Ghasemi R., Ahmadiani A. (2015) Glycogen synthase kinase-3 beta (GSK-3 $\beta$ ) signaling: implications for Parkinson's disease. *Pharmacol Res*;97:16–26.
9. McCubrey J.A., Steelman L.S., Bertrand F.E., Davis N.M., Sokolosky M., Abrams S.L., Montalto G. *et al.* (2014) GSK-3 as potential target for therapeutic intervention in cancer. *Oncotarget*;5:2881–2911.

10. Medina M., Wandosell F. (2011) Deconstructing GSK-3: the fine regulation of its activity. *Int J Alzheimer's Dis*;1–12.
11. Cuzzocrea S., Crisafulli C., Mazzon E., Esposito E., Muià C., Abdelrahman M., Di Paola R., Thiemermann C. (2006) Inhibition of glycogen synthase kinase-3 $\beta$  attenuates the development of carrageenan-induced lung injury in mice. *Br J Pharmacol*;149:687–702.
12. Verma I.M. (2004) Nuclear factor (NF)- $\kappa$ B proteins: therapeutic targets. *Ann Rheum Dis*;63:ii57–ii61.
13. Cheng Y.L., Wang C.Y., Huang W.C., Tsai C.C., Chen C.L., Shen C.F., Chi A.Y., Lin C.F. (2009) Staphylococcus aureus induces microglial inflammation via a glycogen synthase kinase 3 $\beta$ -regulated pathway. *Infect Immun*;77:4002–4008.
14. Bao Z., Lim S., Liao W., Lin Y., Thiemermann C., Leung B.P., Wong W.S.F. (2007) Glycogen synthase kinase-3 $\beta$  inhibition attenuates asthma in mice. *Am J Respir Crit Care Med*;176:431–438.
15. Cuzzocrea S., Mazzon E., Di Paola R., Muià C., Crisafulli C., Dugo L., Collin M., Britti D., Caputi A.P., Thiemermann C. (2006) Glycogen synthase kinase-3 $\beta$  inhibition attenuates the degree of arthritis caused by type II collagen in the mouse. *Clin Immunol*;120:57–67.
16. De Sarno P., Axtell R.C., Raman C., Roth K.A., Alessi D.R., Jope R.S. (2008) Lithium prevents and ameliorates experimental autoimmune encephalomyelitis. *J Immunol*;181:338–345.
17. Dugo L., Collin M., Allen D.A., Murch O., Foster S.J., Yaqoob M.M., Thiemermann C. (2006) Insulin reduces the multiple organ injury and dysfunction caused by coadministration of lipopolysaccharide and peptidoglycan independently of blood glucose: role of glycogen synthase kinase-3 $\beta$  inhibition. *Crit Care Med*;34:1489–1496.
18. Dugo L., Collin M., Allen D.A., Patel N.S., Bauer I., Mervaala E.M., Louhelainen M., Foster S.J., Yaqoob M.M., Thiemermann C. (2005) GSK-3 $\beta$  inhibitors attenuate the organ injury/dysfunction caused by endotoxemia in the rat. *Crit Care Med*;33:1903–1912.
19. Huang W.C., Lin Y.S., Wang C.Y., Tsai C.C., Tseng H.C., Chen C.L., Lu P.J., Chen P.S., Qian L., Hong J.S., Lin C.F. (2009) Glycogen synthase kinase-3 negatively regulates anti-inflammatory interleukin-10 for lipopolysaccharide-induced iNOS/NO biosynthesis and RANTES production in microglial cells. *Immunology*;128:e275–e286.
20. Martin M., Rehani K., Jope R.S., Michalek S.M. (2005) Toll-like receptor-mediated cytokine production is differentially regulated by glycogen synthase kinase 3. *Nat Immunol*;6:777–784.
21. Takada Y., Fang X., Jamaluddin M.S., Boyd D.D., Aggarwal B.B. (2004) Genetic deletion of glycogen synthase kinase-3 $\beta$  abrogates activation of I $\kappa$ B $\alpha$  kinase, JNK, Akt, and p44/p42 MAPK but potentiates apoptosis induced by tumor necrosis factor. *J Biol Chem*;279:39541–39554.
22. Whittle B.J.R., Varga C., Pósa A., Molnár A., Collin M., Thiemermann C. (2006) Reduction of experimental colitis in the rat by inhibitors of glycogen synthase kinase-3 $\beta$ . *Br J Pharmacol*;147:575–582.
23. Jope R.S., Yuskaitis C.J., Beurel E. (2007) Glycogen synthase kinase-3 (GSK3): inflammation, diseases, and therapeutics. *Neurochem Res*;32:577–595.
24. Shafi S., Mahboob Alam M., Mulakayala N., Mulakayala C., Vanaja G., Kalle A.M., Pallu R., Alam M.S. (2012) Synthesis of novel 2-mercapto benzothiazole and 1,2,3-triazole based bis-heterocycles: their anti-inflammatory and anti-nociceptive activities. *Eur J Med Chem*;49:324–333.
25. Haider S., Alam M.S., Hamid H., Shafi S., Nargotra A., Mahajan P., Nazreen S., Kalle A.M., Kharbanda C., Ali Y., Alam A., Panda A.K. (2013) Synthesis of novel 1,2,3-triazole based benzoxazolones: their TNF-alpha based molecular docking with in-vivo anti-inflammatory, antinociceptive activities and ulcerogenic risk evaluation. *Eur J Med Chem*;70:579–588.
26. Haider S., Alam M.S., Hamid H., Shafi S., Dhulap A., Hussain F., Alam P., Umar S., Pasha M.A.Q., Bano S., Nazreen S., Ali Y., Kharbanda C. (2014) Synthesis of novel 2-mercaptobenzoxazole based 1,2,3-triazoles as inhibitors of proinflammatory cytokines and suppressors of COX-2 gene expression. *Eur J Med Chem*;81:204–217.
27. Flouzat C., Bresson Y., Mattio A., Bonnet J., Guillaumet G. (1993) Novel nonopioid non-antiinflammatory analgesics: 3-(aminoalkyl)- and 3-[(4-aryl-1-piperazinyl)alkyl]oxazolo[4,5-b]pyridin-2(3H)-ones. *J Med Chem*;36:497–503.
28. Marie-Claude V., Patricia J., Marie-Laure B., Laurence S., Gérald G. (1997) Acylation of oxazolo[4,5-b]pyridin-2(3H)-ones, 2-phenyloxazolo[4,5-b]pyridines and pyrrolo[2,3-b]pyridin-2(2H)-ones. *Tetrahedron*;53:5159–5168.
29. Viaud M.C., Jamoneau P., Flouzat C., Bizot-Espiard J.G., Pfeiffer B., Renard P., Caignard D.H., Adam G., Guillaumet G. (1995) N-substituted oxazolo[5,4-b]pyridin-2(1H)-ones: a new class of non-opiate antinociceptive agents. *J Med Chem*;38:1278–1286.
30. Savelon L., Bizot-Espiard J.G., Caignard D.H., Pfeiffer B., Renard P., Viaud M.C., Guillaumet G. (1998) 6-aminoalkyloxazolo[4,5-b]pyridin-2(3H)-ones: synthesis and evaluation of antinociceptive activity. *Bioorg Med Chem*;6:1963–1973.
31. Gökhan N., Erdogan H., Durlu T., Demirdamar R. (1999) Novel antiinflammatory analgesics: 3-(2-/4-Pyridylethyl)-benzoxazolinone and oxazolo[4,5- $\beta$ ]pyridin-2-one derivatives. *Arch Pharm*;332:45–49.
32. Courtois M., Mincheva Z., Andreu F., Rideau M., Viaud-Massuard M.C. (2004) Synthesis and biological evaluation with plant cells of new fosmidomycin analogues containing a benzoxazolone or oxazolopyridinone ring. *J Enzyme Inhib Med Chem*;19:559–565.
33. Schadt O., Dorsch D., Stieber F., Blaukat A. (2011) 2-oxo-3-benzylbenzoxazol-2-one derivatives and related

- compounds as Met kinase inhibitors for the treatment of tumours. *2-oxo-3-benzylbenzoxazol-2-one derivatives and related compounds as Met kinase inhibitors for the treatment of tumours*. US 8431572 B2.
34. Åhlin K., Arvidsson P.I., Huerta F., Yngve U. (2011) Oxazolo[4,5-c]pyridine substituted pyrazine. *Oxazolo [4,5-c]pyridine substituted pyrazine*. US20110118275.
  35. Agalave S.G., Maujan S.R., Pore V.S. (2011) Click chemistry: 1,2,3-triazoles as pharmacophores. *Chem Asian J*;6:2696–2718.
  36. Shakeelu R., Masoodur R., Tripathi V.K., Singh J., Ara T., Koul S., Farooq S., Kaul A. (2014) Synthesis and biological evaluation of novel isoxazoles and triazoles linked 6-hydroxycoumarin as potent cytotoxic agents. *Bioorg Med Chem Lett*;24:4243–4246.
  37. Olesen P.H., Sørensen A.R., Ursø B., Kurtzhals P., Bowler A.N., Ehrbar U., Hansen B.F. (2003) Synthesis and *in vitro* characterization of 1-(4-aminofurazan-3-yl)-5-dialkylaminomethyl-1H-[1,2,3]triazole-4-carboxylic acid derivatives. A new class of selective GSK-3 inhibitors. *J Med Chem*;46:3333–3341.
  38. Baki A., Bielik A., Molnár L., Szendrei G., Keserü G.M. (2007) A high throughput luminescent assay for glycogen synthase kinase-3 $\beta$  inhibitors. *Assay Drug Dev Technol*;5:75–83.
  39. Winter C.A., Risley E.A., Nuss G.W. (1962) Carageenin-induced edema in hind paw of the rat as an assay for antiinflammatory drugs. *Proc Soc Exp Biol Med*;111:544–547.
  40. Ferreira S.H. (1979) A new method for measuring variations of rat paw volume. *J Pharm Pharmacol*;31:648.
  41. Ahmad S.F., Bani S., Sultan P., Ali S.A., Bakheet S.A., Attia S.M., Abd-Allah A.R. (2013) TNF-alpha inhibitory effect of *Euphorbia hirta* in rats. *Pharm Biol*;51:411–417.
  42. Wang Z.M., Zhu S.G., Wu Z.W., Lu Y., Fu H.Z., Qian R.Q. (2011) Kirenol upregulates nuclear annexin-1 which interacts with NF-kappaB to attenuate synovial inflammation of collagen-induced arthritis in rats. *J Ethnopharmacol*;137:774–782.
  43. Umar S., Umar K., Sarwar A.H., Khan A., Ahmad N., Ahmad S., Katiyar C.K., Husain S.A., Khan H.A. (2014) *Boswellia serrata* extract attenuates inflammatory mediators and oxidative stress in collagen induced arthritis. *Phytomedicine*;21:847–856.
  44. Ali Y., Alam M.S., Hamid H., Husain A., Shafi S., Dhulap A., Hussain F., Bano S., Kharbanda C., Nazreen S., Haider S. (2015) Design and synthesis of butenolide-based novel benzyl pyrrolones: their TNF-alpha based molecular docking with *in vivo* and *in vitro* anti-inflammatory activity. *Chem Biol Drug Des*;86:619–625.
  45. Polgár T., Baki A., Szendrei G.I., Keserü G.M. (2005) Comparative virtual and experimental high-throughput screening for glycogen synthase kinase-3 $\beta$  inhibitors. *J Med Chem*;48:7946–7959.
  46. Umar S., Zargan J., Umar K., Ahmad S., Katiyar C.K., Khan H.A. (2012) Modulation of the oxidative stress and inflammatory cytokine response by thymoquinone in the collagen induced arthritis in Wistar rats. *Chem Biol Interact*;197:40–46.
  47. Seo W.G., Pae H.O., Oh G.S., Chai K.Y., Kwon T.O., Yun Y.G., Kim N.Y., Chung H.T. (2001) Inhibitory effects of methanol extract of *Cyperus rotundus* rhizomes on nitric oxide and superoxide productions by murine macrophage cell line, RAW 264.7 cells. *J Ethnopharmacol*;76:59–64.
  48. Shukla M., Gupta K., Rasheed Z., Khan K.A., Haqqi T.M. (2008) Bioavailable constituents/metabolites of pomegranate (*Punica granatum* L) preferentially inhibit COX2 activity *ex vivo* and IL-1beta-induced PGE2 production in human chondrocytes *in vitro*. *J Inflamm*;5:9.
  49. Umar S., Kumar A., Sajad M., Zargan J., Ansari M., Ahmad S., Katiyar C.K., Khan H.A. (2013) Hesperidin inhibits collagen-induced arthritis possibly through suppression of free radical load and reduction in neutrophil activation and infiltration. *Rheumatol Int*;33:657–663.
  50. Kim H.G., Han E.H., Jang W.S., Choi J.H., Khanal T., Park B.H., Tran T.P., Chung Y.C., Jeong H.G. (2012) Piperine inhibits PMA-induced cyclooxygenase-2 expression through downregulating NF-kappaB, C/EBP and AP-1 signaling pathways in murine macrophages. *Food Chem Toxicol*;50:2342–2348.
  51. Pande V., Ramos M.J. (2005) Structural basis for the GSK-3 $\beta$  binding affinity and selectivity against CDK-2 of 1-(4-aminofurazan-3yl)-5-dialkylaminomethyl-1H-[1,2,3] triazole-4-carboxylic acid derivatives. *Bioorg Med Chem Lett*;15:5129–5135.
  52. Kramer T., Schmidt B., Lo Monte F. (2012) Small-molecule inhibitors of GSK-3: structural insights and their application to Alzheimer's disease models. *Int J Alzheimer's Dis*;2012:32.
  53. Quesada-Romero L., Mena-Ulecia K., Tiznado W., Caballero J. (2014) Insights into the interactions between maleimide derivatives and GSK3 $\beta$  combining molecular docking and QSAR. *PLoS ONE*;9:e102212.
  54. Darshit B.S., Balaji B., Rani P., Ramanathan M. (2014) Identification and *in vitro* evaluation of new leads as selective and competitive glycogen synthase kinase-3beta inhibitors through ligand and structure based drug design. *J Mol Graph Model*;53:31–47.
  55. Akhtar M., Bharatam P.V. (2012) 3D-QSAR and molecular docking studies on 3-anilino-4-arylmaleimide derivatives as glycogen synthase kinase-3 $\beta$  inhibitors. *Chem Biol Drug Des*;79:560–571.
  56. Quesada-Romero L., Caballero J. (2014) Docking and quantitative structure-activity relationship of oxadiazole derivatives as inhibitors of GSK3beta. *Mol Divers*;18:149–159.
  57. Oxford Diffraction Ltd (2007) Xcalibur CCD System. Abingdon, Oxfordshire: Oxford Diffraction Ltd.
  58. Clark R.C., Reid J.S. (1995) The analytical calculation of absorption in multifaceted crystals. *Acta Crystallogr A*;51:887–897.
  59. Saini M.K., Gupta R., Singh S., Hussain F. (2015) Synthesis, crystal structure and catalytic activity of the

guanidinium cation directed nickel(ii)-containing open Wells-Dawson 19-tungstodiarsonate(iii) [ $\{\text{Ni}(\text{H}_2\text{O})_4\}_2\{\text{Na}(\text{H}_2\text{O})\}\text{As}_2\text{W}_{19}\text{O}_{67}(\text{H}_2\text{O})_9$ ]. RSC Adv;5:25273–25278.

60. Bourhis L.J., Dolomanov O.V., Gildea R.J., Howard J.A.K., Puschmann H. (2015) The anatomy of a comprehensive constrained, restrained refinement program for the modern computing environment – Olex2 dissected. Acta Crystallogr A;71:59–75.
61. Sheldrick G.M. (2008) A short history of SHELX. Acta Crystallogr A;64:112–122.
62. Sheldrick G. (2015) SHELXT – Integrated space-group and crystal-structure determination. Acta Crystallogr A;71:3–8.

## Supporting Information

Additional Supporting Information may be found in the online version of this article:

### Appendix S1 Experimental.

**Figure S1** Effects of test compounds, indomethacin and SB216763 on nitric oxide as measured in rat paw homogenate.

**Figure S2** Effects of test compounds, indomethacin and

SB216763 on inflammatory mediators was measured in rat paw homogenate (A) Tumor necrosis factor- $\alpha$  (TNF- $\alpha$ ) (B) Interleukin-1 $\beta$  (IL-1 $\beta$ ) and (C) Interleukin-6 (IL-6).

**Figure S3** (a) The binding mode of **4g** (Grey) is shown in the GSK-3 $\beta$  active site and important residues are highlighted with Silver stick. (b) Ligplot of **4g** with GSK-3 $\beta$  active site (c) The binding mode of **IQ6** (Grey) is shown in the GSK-3 $\beta$  active site and important residues are highlighted with Silver stick. (d) Ligplot of **IQ6** with GSK-3 $\beta$  active site (e) Comparison of **4g** (Cyan) and co-crystal ligand (Dark green) binding mode in the GSK-3 $\beta$  active site.

**Figure S4** Histopathology report of ulcerogenic risk potential of active compounds.

**Figure S5** Crystal structure of **4q**.

**Table S1** Oxazolo[4,5-b]pyridin-2-one based 1,2,3-triazoles and their GSK-3 $\beta$  inhibitory activity.

**Table S2** *In vivo* Anti-inflammatory activity of oxazolo[4,5-b]pyridin-2-one based 1,2,3-triazoles.

**Table S3** *In silico* docking scores with respect to GSK-3 $\beta$  protein target (PDBID:4IQ6).